

# Aortic Curvature Instead of Angulation Allows Improved Estimation of the True Aorto-iliac Trajectory

R.C.L. Schuurmann<sup>a,b,\*</sup>, L. Kuster<sup>a</sup>, C.H. Slump<sup>c</sup>, A. Vahl<sup>d</sup>, D.A.F. van den Heuvel<sup>e</sup>, K. Ouriel<sup>f</sup>, J.-P.P.M. de Vries<sup>b</sup>

<sup>a</sup> Technical Medicine, Faculty of Science and Technology, University of Twente, Enschede, The Netherlands

<sup>b</sup> Department of Vascular Surgery, St. Antonius Hospital, Nieuwegein, The Netherlands

<sup>c</sup> MIRA Institute for Biomedical Technology and Technical Medicine, University of Twente, Enschede, The Netherlands

<sup>d</sup> Department of Vascular Surgery, Onze Lieve Vrouwe Gasthuis, Amsterdam, The Netherlands

<sup>e</sup> Department of Radiology, St. Antonius Hospital, Nieuwegein, The Netherlands

<sup>f</sup> Syntactx, World Trade Center, New York, NY, USA

## WHAT THIS PAPER ADDS

Aortic neck angulation influences the accuracy of endograft placement and long-term endovascular abdominal aortic repair outcome. To date, a uniform angulation measurement method is lacking and the current methods are prone to subjective interpretation and assume a triangular oversimplification of the aortic neck. The present paper introduces and validates a new method that allows uniform assessment of aortic neck curvature along the center lumen line.

**Objective:** Supra- and infrarenal aortic neck angulation have been associated with complications after endovascular aortic aneurysm repair. However, a uniform angulation measurement method is lacking and the concept of angulation suggests a triangular oversimplification of the aortic anatomy. (Semi-)automated calculation of curvature along the center luminal line describes the actual trajectory of the aorta. This study proposes a methodology for calculating aortic (neck) curvature and suggests an additional method based on available tools in current workstations: curvature by digital calipers (CDC).

**Methods:** Proprietary custom software was developed for automatic calculation of the severity and location of the largest supra- and infrarenal curvature over the center luminal line. Twenty-four patients with severe supra- or infrarenal angulations ( $\geq 45^\circ$ ) and 11 patients with small to moderate angulations ( $< 45^\circ$ ) were included. Both CDC and angulation were measured by two independent observers on the pre- and postoperative computed tomographic angiography scans. The relationships between actual curvature and CDC and angulation were visualized and tested with Pearson's correlation coefficient. The CDC was also fully automatically calculated with proprietary custom software. The difference between manual and automatic determination of CDC was tested with a paired Student *t* test. A *p*-value was considered significant when two-tailed  $\alpha < .05$ .

**Results:** The correlation between actual curvature and manual CDC is strong (.586–.962) and even stronger for automatic CDC (.865–.961). The correlation between actual curvature and angulation is much lower (.410–.737). Flow direction angulation values overestimate CDC measurements by 60%, with larger variance. No significant difference was found in automatically calculated CDC values and manually measured CDC values.

**Conclusion:** Curvature calculation of the aortic neck improves determination of the true aortic trajectory. Automatic calculation of the actual curvature is preferable, but measurement or calculation of the curvature by digital calipers is a valid alternative if actual curvature is not at hand.

© 2015 European Society for Vascular Surgery. Published by Elsevier Ltd. All rights reserved.

Article history: Received 16 April 2015, Accepted 2 September 2015, Available online 27 October 2015

**Keywords:** Abdominal aortic aneurysm, Computing methodologies, Endovascular procedures, Stents

## INTRODUCTION

During the last decade endovascular aneurysm repair (EVAR) has become the preferred treatment modality for infrarenal aortic aneurysms (AAA), with superior short-term results compared with open surgery.<sup>1</sup> However, long-term outcome is highly dependent on patient selection and procedure planning.<sup>2,3</sup> In challenging aortic neck anatomy, EVAR has been associated with substantial complications, including endograft migration and type Ia endoleaks.

\* Corresponding author. St. Antonius Hospital, Department of Surgery, PO Box 2500, 3430 EM Nieuwegein, The Netherlands.

E-mail address: [richte.schuurmann@gmail.com](mailto:richte.schuurmann@gmail.com) (R.C.L. Schuurmann).

1078-5884/© 2015 European Society for Vascular Surgery. Published by Elsevier Ltd. All rights reserved.

<http://dx.doi.org/10.1016/j.ejvs.2015.09.008>

Among hostile neck anatomy characteristics, both suprarenal angulation ( $>45^\circ$ ) and infrarenal angulation ( $>60^\circ$ ) are important.<sup>4–9</sup>

Despite inclusion of large numbers of patients in previous EVAR studies, it is difficult to determine the influence of each individual aortic neck characteristic on post-EVAR complications. One of the difficulties is the lack of a standardized measuring methodology. Angulation is measured in different ways, compromising reliable comparisons between studies as well as the interpretation of endograft manufacturers' instructions for use (IFU).

Over the past 10 years, more and more preoperative sizing and planning has been based on the center luminal line (CLL) reconstructions with the use of a 3D workstation. To determine supra- and infrarenal angulation, 3D workstations offer the option of measuring the angle between the flow direction from the suprarenal aorta to the aortic neck and from the aortic neck to the aneurysm sac along the CLL, respectively. This method is based on the 2D method described by van Keulen and coworkers, and adapted for measuring in three dimensions along the CLL.<sup>10</sup> The angulation measurement over the CLL is referred to as the flow direction angulation method (FDAM).

By using the FDAM, the maximum angle at the crossing of two flow lines is measured. For gentle curvature, the intersection is located far from the center luminal line, and therefore it overestimates the true aortic curvature. Also, measuring the change in flow direction may underestimate the risk factors for EVAR, as tortuous segments will be ignored.

In the present study, a new method is proposed that describes the actual curve of the aorta that is followed by

the endograft during deployment throughout the entire aortic neck and into the aneurysm. A better term to describe this aortic trajectory would be curvature instead of angulation, as angulation suggests a triangular oversimplification of the aortic anatomy. Curvature takes into account not only the severity of the angulation, but also the shape of the trajectory over which the angulation is present. Angulation, contrary to curvature, cannot differentiate between sharp and long curves, while large aortic neck curvature could result in suboptimal endograft deployment (Fig. 1).

In this paper, the method for calculating aortic curvature is described and tested on a cohort of 35 EVAR patients. The curvature is defined by a mathematical formula and will be referred to as "actual curvature." As this formula for actual curvature is not available in all clinically used workstations, a semi-automated measurement method is described that enables aortic curvature measurements with digital calipers, called "curvature by digital calipers" (CDC). The hypothesis is that CDC is a good approximation of the actual (mathematically calculated) curvature. Both angulation by the flow direction method (FDAM) and CDC will be compared with the actual curvature to test this hypothesis.

## METHODS

### Curvature and angulation

The 3mensio workstation (3mensio Vascular 7.0, Medical Imaging BV, Bilthoven, The Netherlands) was used to obtain the CLL at 1 mm increments from the CT scan. This CLL was used to obtain the supra- and infrarenal curvature and angulation. Matlab 2013b (The MathWorks, Natick,

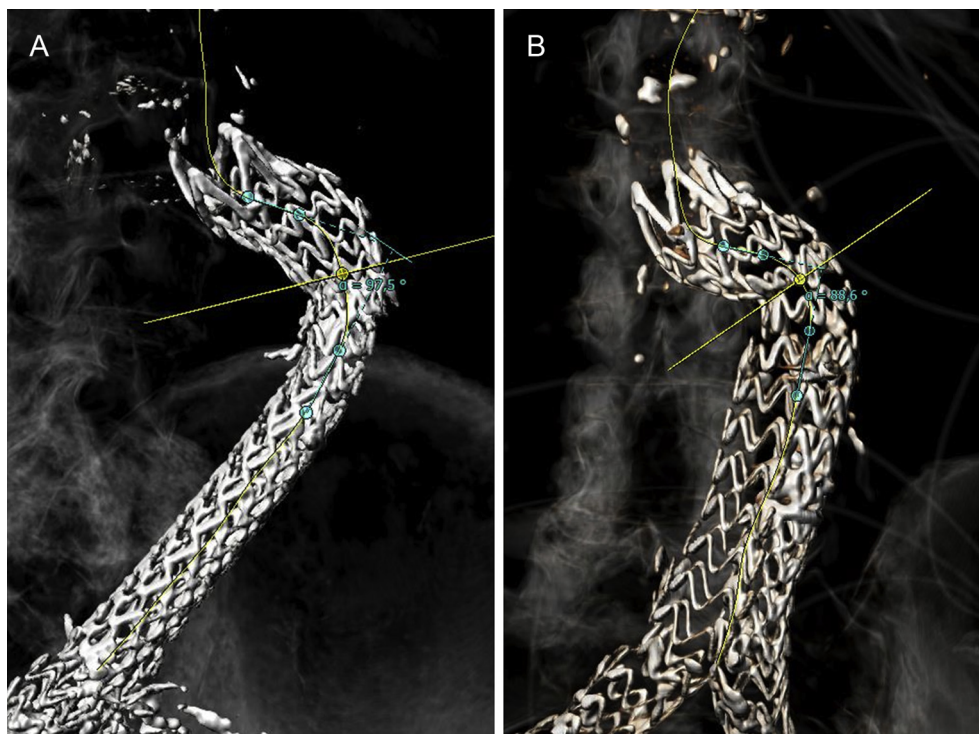


**Figure 1.** Endograft segmentation in two heavily angulated aortas, the angulation is measured with the flow direction angulation method (FDAM). (A) Large angulation ( $97.5^\circ$ ), but low curvature, endograft is correctly deployed. (B) Large angulation ( $88.6^\circ$ ) and large curvature, the endograft is slightly kinked. A lower risk for migration and type Ia endoleaks is suspected in (A) compared with (B).

Massachusetts, USA), software for numerical calculations, visualization and programming, was used to develop customized software to calculate curvature over the CLL.

The actual curvature ( $\kappa$ ) was calculated by numerical computation, using the mathematical definition of extrinsic linear curvature (Equation 1; Fig. 2A).

$$\kappa = \frac{\sqrt{(z''y' - y''z')^2 + (x''z' - z''x')^2 + (y''x' - x''y')^2}}{(x'^2 + y'^2 + z'^2)^{3/2}}, \quad (1)$$

where  $[x, y, z]$  are the CLL Cartesian coordinates, ' = first derivative, '' = second derivative.

Two digital caliper methods were used, one manual and one automated. The digital caliper is an isosceles triangle of three points that can be shifted over the CLL with the cursor of the computer mouse. The CDC is the angle between the three coordinates subtracted from  $180^\circ$ , which is displayed at the screen for each desired location at the CLL (Fig. 2B). The largest suprarenal ( $\gamma$ ) and infrarenal ( $\delta$ ) CDC were measured in the 3mensio workstation by two experienced observers.

The automated Curvature by Digital Calipers (aCDC) was calculated with the customized software. The largest suprarenal ( $\gamma$ ) and infrarenal ( $\delta$ ) aCDC were automatically determined by the software (Fig. 2C).

The angulation (FDAM) was measured in three dimensions by two experienced observers from the 3D CLL in the 3mensio workstation. The suprarenal angle ( $\alpha$ ) was measured between the flow axis of the suprarenal aorta and the flow axis of the aortic neck, the infrarenal angle ( $\beta$ ) was measured between the flow axis of the aortic neck and the flow axis of the aneurysm sac, as is described by Van Keulen and co-workers (Fig. 2D).<sup>10</sup> In case of multiple angles, the maximum angle was chosen. The flow axis was defined by two points on the CLL, marking the inflow and outflow of the segment.

### Software validation

The automatic calculation of maximal curvature by digital calipers was validated by correlating it to the outcome of 35 pre- and postoperative measurements of the curvatures  $\gamma$  and  $\delta$  by digital calipers in 3mensio. The measurements were performed by two experienced observers.

### Patient inclusion

In this study, 35 patients (29 males, mean age  $76 \pm 6$  years) who had undergone elective endovascular repair of an infrarenal aortic aneurysm with an Endurant endoprosthesis (Medtronic, Santa Rosa, CA, USA) were included. Both supra- and infrarenal angulations were calculated on the preprocedural CT-scans with the FDAM. Twenty-four consecutive patients with supra- or infrarenal angulation  $>45^\circ$ , and 11 consecutive patients with milder angulations were selected. The large number of severely angulated aortic necks was chosen because it was hypothesized that angulation measurements will be more difficult in severe angulations and to show the added value of curvature in these complex anatomies. The protocol was approved by the institutional review board.

Mean time interval from the preoperative CT scan to the EVAR procedure was 63 days (1–194), and from surgery to postoperative CT scan was 33 days (13–64).

### CTA scan protocol

CTA images were acquired on a 256 slice CT scanner. Scan parameters were: tube voltage 120 kV, tube current time product 180 mAs pre- and 200 mAs postoperative, distance between slices 0.75 mm, pitch 0.9 mm, collimation  $128 \text{ mm} \times 0.625 \text{ mm}$  pre- and  $16 \text{ mm} \times 0.75 \text{ mm}$  postoperative. Preoperative slice thickness was  $2.1 \pm 1.1 \text{ mm}$ . Postoperative slice thickness was  $1.6 \pm 0.4 \text{ mm}$ . Preoperatively, 100 mL Xenetix300 contrast was administered intravenously in the arterial phase at 4 mL/s, postoperatively 80 mL was administered at 3 mL/s.

### Statistical analysis

Statistical analysis was performed with SPSS v. 22 (IBM Corp, Armonk, NY, USA). A  $p$ -value was considered significant when two-tailed  $\alpha < .05$ . Difference between manual and automatic determination of CDC was tested with the paired Student  $t$  test. Bland-Altman plots were constructed as scatter plots in which the Y axis represented the difference between two paired measurements and the X axis represented the average of these measurements.

### Correlation between actual curvature and measured angulation and curvature

Thirty-five pre- and postoperative measurements of angles  $\alpha$  and  $\beta$  by FDAM and curvatures  $\gamma$  and  $\delta$  by CDC were correlated to the actual curvature for each of the two observers. The relationship between the different methods and the actual curvature was shown in scatter plots and tested with the two-tailed Pearson correlation coefficient.

There are two online supplements to these methods: [Appendix I](#). In vitro validation of curvature calculation over the center luminal line, and [Appendix II](#). Conversion from CDC ( $^\circ$ ) to curvature ( $\text{m}^{-1}$ ).

## RESULTS

Fig. 2 shows an example of the actual curvature, angles  $\alpha$  and  $\beta$  by FDAM, CDC, and aCDC  $\gamma$  and  $\delta$ . All measurements and calculations were performed on the same CLL.

An example of the aCDC versus the actual curvature over the entire trajectory of the abdominal aorta is shown in Fig. 3. This graph shows the curvature over the aortic trajectory from the suprarenal aorta to the bifurcation. The graph also illustrates the location, magnitude (height of peak), and trajectory (width of peak) of curvatures  $\gamma$  and  $\delta$ .

### Validation of aCDC

Pre- and postoperative maximal curvatures  $\gamma$  and  $\delta$  on the CLL of 35 patients were measured by an experienced observer in 3mensio (CDC) and calculated in Matlab (aCDC). The paired  $t$  test showed no significant difference between maximum automatic and measured CDC over any of the

regions (Table 1). The Bland-Altman plot shows a minimal systematic error, suggesting good agreement between the CDC and aCDC (Fig. 4).

### Correlation between angulation and curvature

Table 2 shows the average angulation and curvature, determined by the different methods over the pre- and

postoperative supra- and infrarenal aorta. Suprarenal angulation is reduced by 2% and infrarenal angulation by 19% as a result of the endoprosthesis implantation. Suprarenal curvature is reduced by 16–23% and infrarenal curvature by 28–29%.

Both automated and manual CDC measurements of the maximum curvature are very close to true mathematical

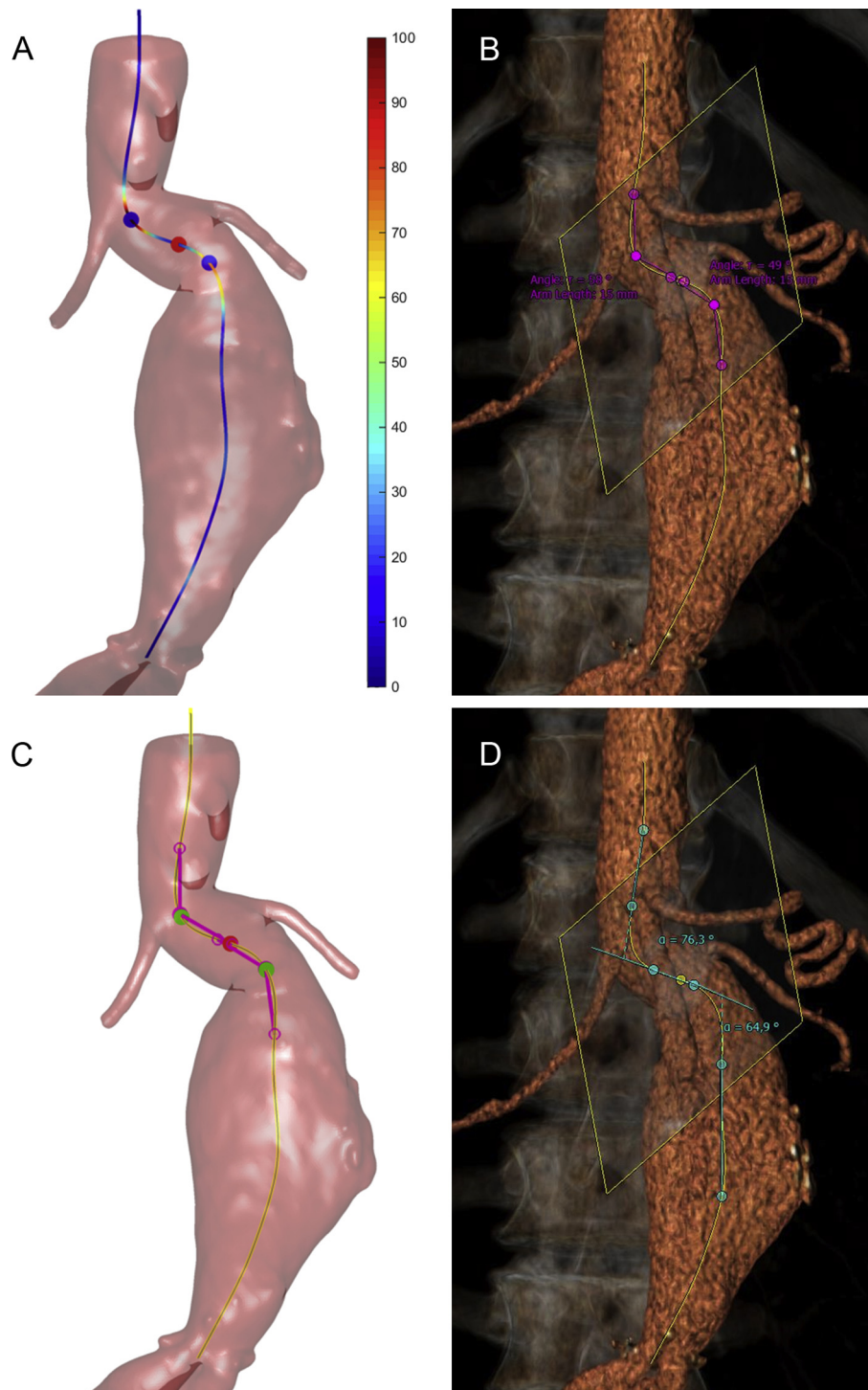


**Figure 2.** Example of angulation and curvature measurements and calculations on a pre-EVAR CTA scan; the orifice of the lowermost renal artery is marked by the yellow plane. (A) Automatic calculation of actual curvature ( $\gamma = 125 \text{ m}^{-1}$ ;  $\delta = 76 \text{ m}^{-1}$ ); the colors indicate the degree of curvature, blue dots mark the location of the largest curvatures. (B) Measured angulation by flow direction in 3mensio ( $\alpha = 76.3^\circ$ ;  $\beta = 64.9^\circ$ ). (C) Measured curvature by digital calipers ( $\gamma = 58^\circ$ ;  $\delta = 49^\circ$ ). (D) Automatically calculated curvatures by digital calipers ( $\gamma = 58^\circ$ ;  $\delta = 49^\circ$ ); the red dot marks the baseline, green dots mark the measured locations of the largest curvatures.

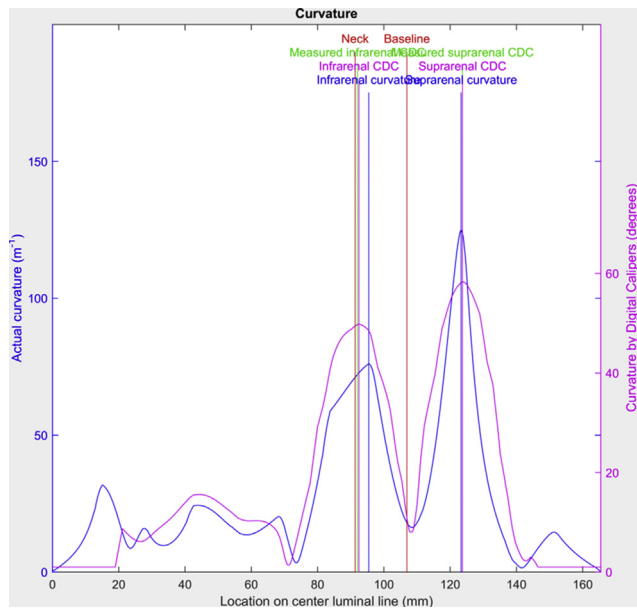


**Figure 3.** Example of actual curvature (blue, in  $m^{-1}$ ) versus automatically calculated aCDC (purple, in  $^{\circ}$ ) over the CLL of the same patient as in Fig. 2. Left to right equals caudal to cranial with the aortic bifurcation set to 0, and locations of the caudal end of the neck (Neck) and orifice of the lowest renal artery (Baseline) are marked. For correct scaling, the conversion factor 1:1.8 is used. The digital calipers closely follow the actual curvature.

midline curvature (Fig. 5A,B; Table 3). The correlation between the actual curvature and the CDC is strong (.586–.962) and even stronger for the aCDC (.865–.961). The correlation between the actual curvature and the FDAM is much lower (.410–.737; Fig. 5C; Table 3). Flow direction angles overestimate CDC by 60% on average, and vary substantially (Fig. 5D).

## DISCUSSION

Measuring or calculating aortic curvature instead of angulation has four advantages:

- 1 Measurements and calculations are performed entirely on the CLL.
- 2 Curvature is calculated over all CLL coordinates, which enables software manufacturers to include calculation of maximum as well as average curvature over specific aortic segments, such as suprarenal aorta, aortic neck, aneurysm, aortic bifurcation, and common iliac artery.
- 3 Distance of the largest curvature from baseline (lowest renal artery) can be measured over the CLL, which enables comparison of the largest curvature location

**Table 1.** Association between automatic and measured largest curvature by digital calipers.

	Automatic mean (SD)	Measured mean (SD)	% Difference	Paired <i>t</i> test <i>p</i> -value
Pre-EVAR, $\gamma$ ( $^{\circ}$ )	32.4 (15.7)	32.5 (15.7)	0.14	.582
Pre-EVAR, $\delta$ ( $^{\circ}$ )	41.9 (14.2)	41.9 (14.1)	0.03	.897
Post-EVAR, $\gamma$ ( $^{\circ}$ )	26.9 (13.6)	27.2 (13.5)	0.95	.056
Post-EVAR, $\delta$ ( $^{\circ}$ )	30.1 (12.7)	30.1 (12.7)	0.16	.490

between multiple follow-up CTA scans. This is useful for proper quantification of eventual displacement of the largest curvature over time and changes in the proximal part of the endograft over time.

4. In a tortuous aorta, multiple relevant curvatures can be measured and displayed, potentially increasing insight into the risks of endovascular repair over long term follow-up.

Despite the essence of a robust and validated measurement method for aortic angulation, multiple methods have been described and are used in clinical practice, each with benefits and limitations.

In 1997, Ahn et al. were the first to describe a classification of aortic angulation.<sup>11</sup> They proposed measurement of the “largest angle,” but did not describe how this angle should be measured. Chaikof and colleagues specified that the suprarenal angle ( $\alpha$ ) should be measured between the flow axis of the suprarenal and infrarenal aortic neck and the infrarenal angle ( $\beta$ ) between the flow axis of the infrarenal neck and the aneurysm body.<sup>3</sup> Van Keulen et al. included the use of a 3D workstation to define angulation  $\alpha$  and  $\beta$ .<sup>10</sup> However, their method was still dependent on the visual interpretation of the largest angle, which might lead to substantial inter-rater variability and the possibility of misinterpreting the location of the largest angle. Furthermore, their method is still based on two-dimensional angulation measurements, often underestimating or overestimating tortuous aorta segments. To reduce the errors of two-dimensional measurements, the method of Van Keulen was adapted to a 3D measurement technique, available in the 3mensio workstation.

Ouriel et al. described a different way of defining aortic angulation.<sup>12</sup> They calculate the angle between fixed points on the aorta CLL. The suprarenal angulation is measured between the orifice of the celiac trunk, the orifice of the lowermost renal artery, and the proximal aspect of the aneurysm sac. The infrarenal angulation is measured between the orifice of the lowermost renal artery, the proximal aspect of the aneurysm sac, and the aortic bifurcation. Despite this method being less susceptible to inter-rater variability than other methods, tortuous segments not located in the inferior renal orifice or the proximal end of the aneurysm sac are not measured, while these segments could contribute to accurate procedure planning or risk analysis for patient outcome.

The variety in measured angles by these different methods influences the interpretation of endograft manufacturers’ instruction for use (IFU). Incorrect interpretation of the IFU could lead to unintentional treatment of patients outside the IFU, or unnecessary open procedures in patients fit for endovascular repair.

This is the first study to describe methods for abdominal aortic curvature measurements. It is hypothesized that procedure success, endograft migration, type Ia endoleak prevalence, and endograft kinking are associated with curvature, rather than with angulation. Fig. 1 shows an example of potential endograft kinking in a postoperative scan in a highly curved aorta, whereas an aorta with similar angulation but lower curvature shows no signs of kinking.

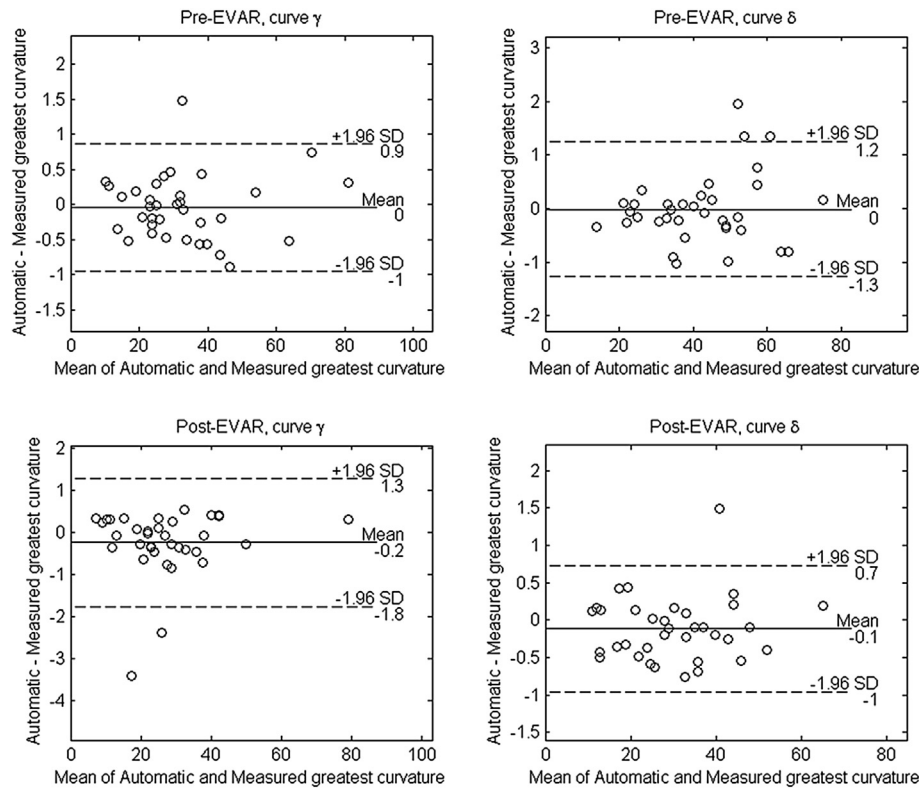


**Figure 4.** Bland-Altman plots of automatic versus measured largest curvature by digital calipers.

The hypothesis of increased risk for migration is supported by findings of Figueroa et al.<sup>13</sup> They show how the increase in aortic curvature leads to higher displacement forces in a 3D computational analysis.

Evidence that curvature is superior to angulation in predicting aortic neck-related adverse events can only be assessed through analysis of clinical data. An other study by our group compared 64 patients who developed intraoperative type IA endoleaks with 79 control participants without early or late neck-related complications. Predictive value of curvature was compared with supra- and infrarenal angulation, neck tortuosity index, and other neck characteristics, including neck length, neck diameter, maximum aneurysm sac diameter, and calcium and thrombus load in the aortic neck. Multivariate regression analysis identified calcification circumference in the aortic neck ( $p = .020$ ) and curvature over the juxtarenal aortic neck ( $p = .039$ ), curvature over the aneurysm sac ( $p = .048$ ) and curvature over the terminal aorta ( $p = .002$ ) as significant predictors for intraoperative type IA endoleak. Suprarenal and infrarenal angulation and aortic neck tortuosity index were no significant predictors.<sup>14</sup>

When it comes to procedure planning, inaccurate assessment of aortic tortuosity can result in underestimation of the true aorta length. This occurs when the stiff endograft

straightens the tortuosity and the angulation is transposed to suprarenal and/or iliac regions. Visualization of the entire aortic tortuosity will be helpful in interpreting the risk for aortic straightening. The overview of the number of curves and their severity are also of great value in preventing physicians for overlooking relevant curvatures. This option, however, is only available for automatic curvature calculation, which is not incorporated in current 3D workstations.

Curvature is a mathematical expression, and can be numerically calculated over the CLL coordinates. The current software can be easily included in any CLL-based workstation at very low costs. Moreover, other commercially available workstations do have some sort of curvature calculations incorporated, which is free of charge.

A strong correlation was seen between the actual curvature and the CDC (Table 3; Fig. 5A), suggesting that digital calipers give a good representation of the actual curvature and therefore are a decent alternative for actual curvature calculation if this is not available. As the digital calipers measure the curvature in a triangular orientation over a distance of 30 mm, sharp curves (narrow peaks in Fig. 3) are smoothed. CDC values depend on the length of the caliper arms. Reducing the caliper arm length would better follow the curve of the CLL, but will also result in smaller curvature values, including more noise. Because exact curvature

**Table 2.** Average pre- and post-EVAR maximum curvature and angulation over the supra- and infrarenal aorta ( $n = 35$ ).

	Actual curvature ( $m^{-1}$ ) mean (SD)	aCDC ( $^{\circ}$ ) mean (SD)	CDC ( $^{\circ}$ ) mean (SD)	Angulation ( $^{\circ}$ ) mean (SD)
Pre-EVAR, $\gamma/\alpha$	62.7 (42.0)	32.4 (15.7)	32.5 (15.7)	43.2 (21.5)
Pre-EVAR, $\delta/\beta$	77.7 (32.3)	41.9 (14.2)	41.9 (14.1)	66.6 (19.3)
Post-EVAR, $\gamma/\alpha$	48.0 (30.0)	26.9 (13.6)	27.2 (13.5)	42.4 (21.8)
Post-EVAR, $\delta/\beta$	55.3 (32.7)	30.1 (12.7)	30.1 (12.7)	53.8 (21.4)

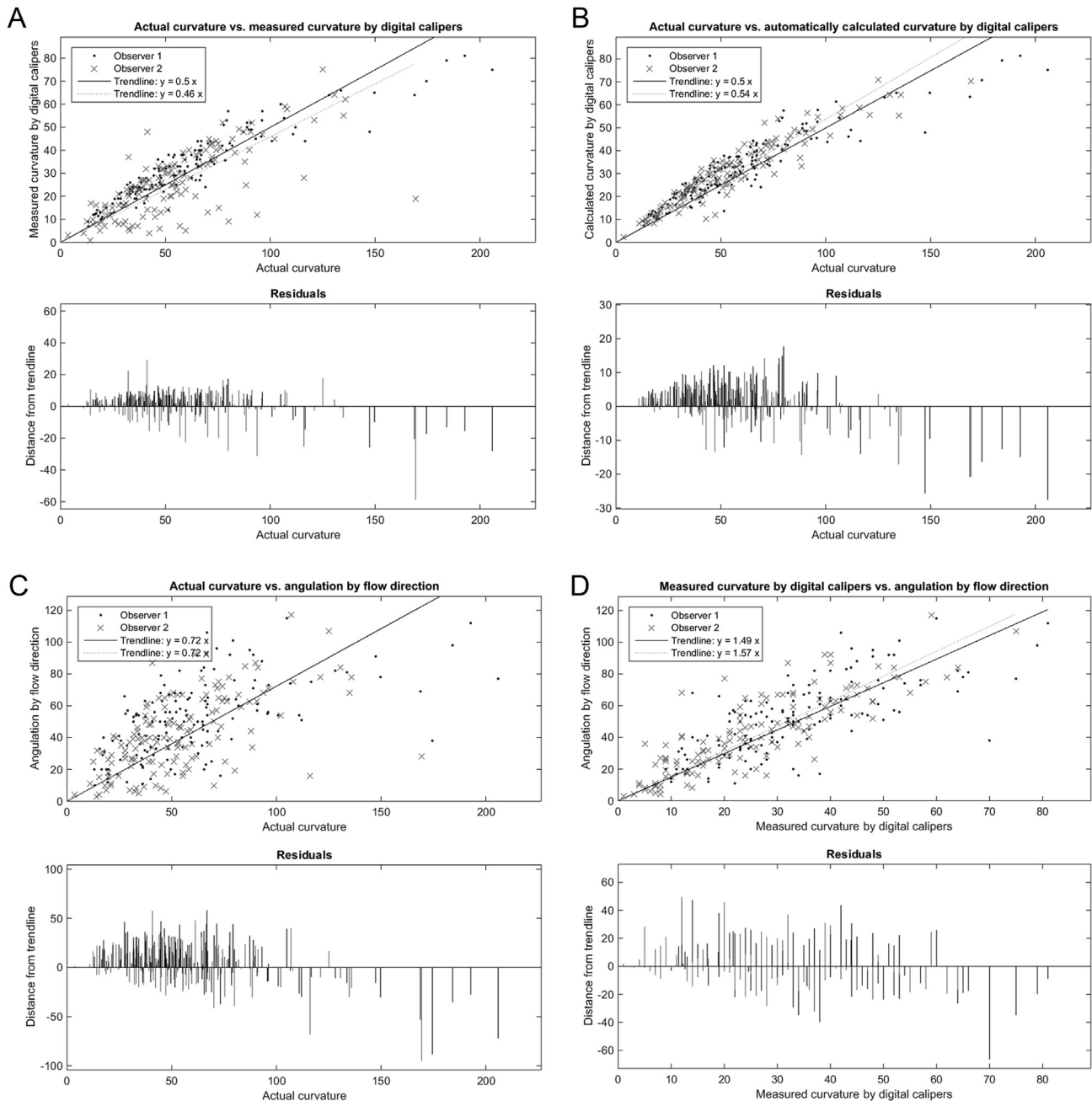


**Figure 5.** Scatter plots of actual curvature versus CDC and FDAM. Measurements by two observers, pre- and postoperative values of supra- and infrarenal aortic neck are combined. (A) Actual curvature versus measured curvature by digital calipers. (B) Actual curvature versus automatically calculated curvature by digital calipers. (C) Actual curvature versus angulation by flow direction. (D) Angulation by flow direction versus measured curvature by digital calipers.

measurement may not be clinically relevant, as long as the measurements provide useful information for procedure planning, improve clinical outcome, and the measurement procedure is fast, easy to use, and reproducible, the exact length of the caliper arms is not of importance. More important, however, is standardization of techniques. The use of a standardized arm length of 15 mm is recommended, which correlates well with the actual curvature and results in curvature values that are easy to interpret. The Tortuosity Angle tool with 15 mm arms, available in the 3mensio workstation, is a good tool for measuring CDC. Other companies may offer similar utilities, but these have not been tested as part of this study.

The locations of curvatures  $\gamma$  and  $\delta$  in relation to the upper and lower renal arteries and the begin of the aneurysm are also important. The proprietary custom software, designed in Matlab, provides an overview of these relations (Fig. 3). Future research is needed to relate the magnitude and location of curvature to procedure success and long-term complications. The effect of aorta straightening, accuracy of post-EVAR endograft placement in angulated aortas, and endograft sealing are also subjects of interest for further research.

The proposed methodology for curvature measurements instead of angulation has two limitations. First, curvature is calculated at every point of the CLL. Reliability of the curvature calculations depends on the correctness of the CLL. If

**Table 3.** Correlation of the actual curvature and the curvature by digital calipers (automatic and manual) and the angulation by flow direction.

		Observer 1		Observer 2	
		Pearson's CC	Significance	Pearson's CC	Significance
Automatic curvature by digital calipers	Pre-EVAR, $\gamma$ ( $^{\circ}$ )	.953	.000	.934	.000
	Pre-EVAR, $\delta$ ( $^{\circ}$ )	.865	.000	.939	.000
	Post-EVAR, $\gamma$ ( $^{\circ}$ )	.958	.000	.961	.000
	Post-EVAR, $\delta$ ( $^{\circ}$ )	.902	.000	.932	.000
Manual curvature by digital calipers	Pre-EVAR, $\gamma$ ( $^{\circ}$ )	.952	.000	.759	.000
	Pre-EVAR, $\delta$ ( $^{\circ}$ )	.874	.000	.857	.000
	Post-EVAR, $\gamma$ ( $^{\circ}$ )	.962	.000	.586	.000
	Post-EVAR, $\delta$ ( $^{\circ}$ )	.902	.000	.785	.000
Angulation by flow direction	Pre-EVAR, $\alpha$ ( $^{\circ}$ )	.521	.001	.711	.000
	Pre-EVAR, $\beta$ ( $^{\circ}$ )	.410	.014	.651	.000
	Post-EVAR, $\alpha$ ( $^{\circ}$ )	.737	.000	.431	.010
	Post-EVAR, $\beta$ ( $^{\circ}$ )	.612	.000	.633	.000

the CLL is misplaced, it will influence the accuracy of the curvature measurements. To reduce this limitation, the CLL should be placed with care in the center of the lumen. This may require some extra planning time.

Second, clinical use of actual curvature measurements has not been published so far. It requires implementation of the curvature calculation software in clinical workstations. Only then can the method be standardized for uniform reporting.

## CONCLUSION

Proper and consistent measurement of aortic (neck) angulation is difficult. It assumes linear, angulated neck configurations, which is often not a true representation of the aortic anatomy. In the current study curvature is calculated instead of angulation. Curvature provides information about the entire aortic trajectory, including severity of angulation. Actual curvature calculation is the most accurate means of representing aortic curvature, but if this option is not available in the workstation, CDC can be measured instead. The current analysis documented a high correlation between CDC and the actual curvature. As the measured CDC is dependent on the caliper arm length, a consensus is needed about the arm length. Until such a consensus is available, an arm length of 15 mm is proposed. This methodology should provide a standardized method of expressing the true aortic trajectory and one that does not assume a linear angular configuration at the aortic neck. This novel technique holds potential to improve the predictive value of aortic neck measurement for identifying those patients at greatest risk for proximal neck complications after endovascular aneurysm repair.

## CONFLICT OF INTEREST

None.

## FUNDING

None.

## APPENDIX A. SUPPLEMENTARY DATA

Supplementary data related to this article can be found at <http://dx.doi.org/10.1016/j.ejvs.2015.09.008>.

## REFERENCES

- 1 Stather PW, Sayers RD, Cheah A, Wild JB, Bown MJ, Choke E. Outcomes of endovascular aneurysm repair in patients with hostile neck anatomy. *Eur J Vasc Endovasc Surg* 2012;**44**(6):556–61.
- 2 Chaikof EL, Blankensteijn JD, Harris PL, Fillinger MF, Matsumura JS, Rutherford RB, et al. Reporting standards for endovascular aortic aneurysm repair. *J Vasc Surg* 2002;**35**(5):1048–60.
- 3 Chaikof EL, Fillinger MF, Matsumura JS, Rutherford RB, White GH, Blankensteijn JD, et al. Identifying and grading factors that modify the outcome of endovascular aortic aneurysm repair. *J Vasc Surg* 2002;**35**(5):1061–6.
- 4 Dillavou ED, Muluk SC, Rhee RY, Tzeng E, Woody JD, Gupta N, et al. Does hostile neck anatomy preclude successful endovascular aortic aneurysm repair? *J Vasc Surg* 2003;**38**(4):657–63.
- 5 Boulton M, Babidge W, Maddern G, Barnes M, Fitridge R. Predictors of success following endovascular aneurysm repair: mid-term results. *Eur J Vasc Endovasc Surg* 2006;**31**(2):123–9.
- 6 Hobo R, Kievit J, Leurs LJ, Buth J. Influence of severe infrarenal aortic neck angulation on complications at the proximal neck following endovascular AAA repair: a EUROSTAR study. *J Endovasc Ther* 2007;**14**(1):1–11.
- 7 Van Herwaarden JA, van de Pavoordt EDWM, Waasdorp EJ, Vos JA, Overtom TT, Kelder JC, et al. Long-term single-center results with AneurRx endografts for endovascular abdominal aortic aneurysm repair. *J Endovasc Ther* 2007;**14**(3):307–17.
- 8 Wyss TR, Dick F, Brown LC, Greenhalgh RM. The influence of thrombus, calcification, angulation, and tortuosity of attachment sites on the time to the first graft-related complication after endovascular aneurysm repair. *J Vasc Surg* 2011;**54**(4):965–71.
- 9 De Vries J-PPM. The proximal neck: the remaining barrier to a complete EVAR world. *Semin Vasc Surg* 2012;**25**(4):182–6.
- 10 Van Keulen JW, Moll FL, Tolenaar JL, Verhagen HJM, van Herwaarden JA. Validation of a new standardized method to measure proximal aneurysm neck angulation. *J Vasc Surg* 2010;**51**(4):821–8.
- 11 Ahn SS, Rutherford RB, Johnston KW, May J, Veith FJ, Baker JD, et al. Reporting standards for infrarenal endovascular abdominal aortic aneurysm repair. *J Vasc Surg* 1997;**25**(2):405–10.
- 12 Ouriel K, Tanquilut E, Greenberg RK, Walker E. Aortiliac morphologic correlations in aneurysms undergoing endovascular repair. *J Vasc Surg* 2003;**38**:323–8.
- 13 Figueroa CA, Taylor CA, Yeh V, Chiou AJ, Zarins CK. Effect of curvature on displacement forces acting on aortic endografts: a 3-dimensional computational analysis. *J Endovasc Ther* 2009;**16**(3):284–94.



14 Schuurmann RCL, Ouriel K, Muhs BE, Jordan Jr WD, Ouriel R, Boersen JT, et al. Aortic curvature as a predictor of intra-

operative type IA endoleak. *J Vasc Surg* 2015;1–7. <http://dx.doi.org/10.1016/j.jvs.2015.08.110>.

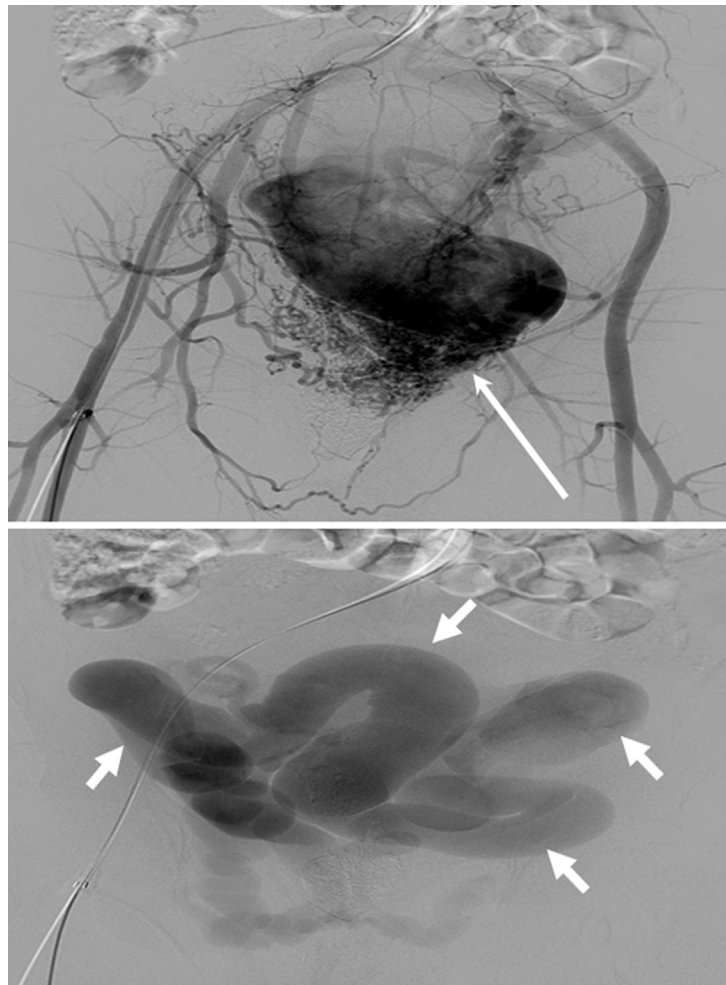
*Eur J Vasc Endovasc Surg* (2016) 51, 224

## COUP D'OEIL

# Enormous Intra-abdominal Arteriovenous Malformation

J. Rodriguez-Padilla, J. De Haro \*

Hospital Universitario Getafe, Madrid, Spain



A 34 year old, otherwise healthy, male was admitted with abdominal pain. Angiography revealed a large abdominal and pelvic arteriovenous malformation (AVM) with huge partially thrombosed aneurysmal abdominal and pelvic veins (short arrows), and multiple high flow arteriovenous shunts forming a nidus of about 5 cm dependent on the hemorrhoidal and bilateral hypogastric arteries (long arrow). The patient was unsuccessfully treated by venous embolization with Onyx 18 and anticoagulated long term to prevent embolism. Intra-abdominal AVMs are infrequent, sporadic, and rarely reported. Presumed to be congenital, these cases rarely present with such huge dimensions.

\* Corresponding author. Hospital Universitario Getafe, Madrid, Spain.

E-mail address: [deharojoaquin@yahoo.es](mailto:deharojoaquin@yahoo.es) (J. De Haro).

1078-5884/© 2015 European Society for Vascular Surgery. Published by Elsevier Ltd. All rights reserved.

<http://dx.doi.org/10.1016/j.ejvs.2015.11.003>